

Diy mobile phone jammer circuit | mobile phone jammer low price

[Home](#)

>

[mobile phone jammer dealers in kerala](#)

>

diy mobile phone jammer circuit

- [advanced mobile phone signal jammer with highlow o](#)
- [advantages of mobile phone jammer](#)
- [buy mobile phone jammer](#)
- [electronic mobile phone jammer](#)
- [gps mobile phone jammer abstract judgment](#)
- [gps mobile phone jammer abstract request](#)
- [gps mobile phone jammer factory](#)
- [gps mobile phone jammer for sale](#)
- [gps mobile phone jammer laws](#)
- [how can i make a mobile phone jammer](#)
- [mini portable mobile phone signal jammer](#)
- [mobile phone jammer Manitoba](#)
- [mobile phone jammer New Brunswick](#)
- [mobile phone and gps jammer china](#)
- [mobile phone gps jammer app](#)
- [mobile phone gps jammer yakima](#)
- [mobile phone jammer australia](#)
- [mobile phone jammer circuit pdf](#)
- [mobile phone jammer cost](#)
- [mobile phone jammer dealers](#)
- [mobile phone jammer dealers in kerala](#)
- [mobile phone jammer detector](#)
- [mobile phone jammer Dieppe](#)
- [mobile phone jammer for home](#)
- [mobile phone jammer in hyderabad](#)
- [mobile phone jammer in uk](#)
- [mobile phone jammer ireland](#)
- [mobile phone jammer Kawartha Lakes](#)
- [mobile phone jammer manufacturer](#)
- [mobile phone jammer Melville](#)
- [mobile phone jammer Mercier](#)
- [mobile phone jammer Nottingham](#)
- [mobile phone jammer overview](#)
- [mobile phone jammer Penticton](#)
- [mobile phone jammer Port Colborne](#)
- [mobile phone jammer price in india](#)

- [mobile phone jammer Prince Edward County](#)
- [mobile phone jammer Prince Rupert](#)
- [mobile phone jammer Steinbach](#)
- [mobile phone jammer Thurso](#)
- [mobile phone jammer Trail](#)
- [mobile phone jammer York](#)
- [mobile phone jammers in pakistan](#)
- [mobile phone signal jammer with pre scheduled time](#)
- [mobile phone signal jammer with remote control](#)
- [mobilephonejammers](#)
- [office mobile phone jammer](#)
- [phone mobile jammer yakima](#)
- [raspberry pi mobile phone jammer](#)
- [where can i get a mobile phone jammer](#)

Permanent Link to Innovation: Under Cover
2021/04/07

Synthetic-Aperture GNSS Signal Processing By Thomas Pany, Nico Falk, Bernhard Riedl, Carsten Stöber, Jón O. Winkel, and Franz-Josef Schimpl INNOVATION INSIGHTS by Richard Langley A SYNTHETIC APERTURE? WHAT'S THAT? Well, an aperture in optics is just a hole or opening through which light travels. Those of us into photography know that the amount of light reaching the camera's imaging sensor is controlled by the shutter speed and the size of the lens opening or aperture (called the f-stop). And a correct combination of the aperture setting and shutter speed results in a correct exposure. For an optical telescope, its aperture is the diameter of its main, light-gathering lens or mirror. A larger aperture gives a sharper and brighter view or image. In the radio part of the electromagnetic spectrum, the term aperture refers to the effective collecting (or transmitting) area of an antenna. The gain of the antenna is proportional to its aperture and its beamwidth or resolution is inversely proportional to it. Astronomers, whether using optical or radio telescopes, often seek higher and higher resolutions to see more detail in the objects they are investigating. Conventionally, that means larger and larger telescopes. However, there are limits to how large a single telescope can be constructed. But by combining the light or radio signals from two or more individual telescopes, one can synthesize a telescope with a diameter equal to the baseline(s) connecting those telescopes. The approach is known as interferometry. It was first tried in the optical domain by the American physicist Albert Michelson who used the technique to measure the diameter of the star Betelgeuse. Radio astronomers developed cable- and microwave-connected interferometers and subsequently they invented the technique of very long baseline interferometry (VLBI) where atomic-clock-stabilized radio signals are recorded on magnetic tape and played back through specially designed correlators to form an image. (VLBI has also been used by geodesists to precisely determine the baselines between pairs of radio telescopes even if they are on separate continents.) A similar approach is used in synthetic-aperture radar (SAR). Mounted on an aircraft or satellite, the SAR beam-forming antenna emits pulses of radio waves that are reflected from a target and then coherently combined. The different positions of the SAR, as it moves, synthesize an elongated aperture resulting

in finer spatial resolution than would be obtained by a conventional antenna. But what has all of this got to do with GNSS? In this month's column, we take a look at a novel GNSS signal-processing technique, which uses the principles of SAR to improve code and carrier-phase observations in degraded environments such as under forest canopy. The technique can simultaneously reject multipath signals while maximizing the direct line-of-sight signal power from a satellite. Along with a specially programmed software receiver, it uses either a single conventional antenna mounted, say, on a pedestrian's backpack for GIS applications or a special rotating antenna for high-accuracy surveying. Want to learn more? Read on. "Innovation" is a regular feature that discusses advances in GPS technology and its applications as well as the fundamentals of GPS positioning. The column is coordinated by Richard Langley of the Department of Geodesy and Geomatics Engineering, University of New Brunswick. He welcomes comments and topic ideas. Over the past few years, we have been developing new GNSS receivers and antennas based on an innovative signal-processing scheme to significantly improve GNSS tracking reliability and accuracy under degraded signal conditions. It is based on the principles of synthetic-aperture radar. Like in a multi-antenna phased-array receiver, GNSS signals from different spatial locations are combined coherently forming an optimized synthetic antenna-gain pattern. Thereby, multipath signals can be rejected and the line-of-sight received signal power is maximized. This is especially beneficial in forests and in other degraded environments. The method is implemented in a real-time PC-based software receiver and works with GPS, GLONASS, and Galileo signals. Multiple frequencies are generally supported. The idea of synthetic-aperture processing is realized as a coherent summation of correlation values of each satellite over the so-called beam-forming interval. Each correlation value is multiplied with a phase factor. For example, the phase factor can be chosen to compensate for the relative antenna motion over the beam-forming interval and the resulting sum of the scaled correlation values represents a coherent correlation value maximizing the line-of-sight signal power. Simultaneously, signals arriving from other directions are partly eliminated. Two main difficulties arise in the synthetic-aperture processing. First, the clock jitter during the beam-forming interval must be precisely known. It can either be estimated based on data from all signals, or a stable oscillator can be used. In one of our setups, a modern oven-controlled crystal oscillator with an Allan variance of 0.5×10^{-13} at an averaging period of 1 second is used. Second, the precise relative motion of the antenna during the beam-forming interval must be known. Again it can be estimated if enough sufficiently clean signals are tracked. The antenna trajectory is estimated directly from the correlator values as shown later in this article. In more severely degraded environments, the antenna may be moved along a known trajectory. We are developing a rotating antenna displacement unit. (see FIGURE 1). The rotational unit targets forestry and indoor surveying applications. The relative motion of the antenna is measured with sub-millimeter accuracy. □FIGURE 1. Artist's impression of the synthetic-aperture GNSS system for surveying in a forest. After beam-forming, the code pseudoranges and the carrier phases are extracted and used in a conventional way. That is, they are written into Receiver Independent Exchange (RINEX) format files and standard geodetic software can be used to evaluate them. In the case where the artificial movement antenna is used, the GNSS signal processing removes the known part of the movement from the observations, and the

observations are then like those from a static antenna. As a result, common static positioning algorithms, including carrier-phase ambiguity fixing, can be applied. The presented method therefore prepares the path for GNSS surveying applications in new areas. An important point is the mechanical realization of the antenna movement. This has to be done in a cost-efficient and reliable way. Lubrication-free actuators are used together with magnetic displacement sensors. The sensors are synchronized to the software receiver front end with better than 1 millisecond accuracy. The rotating antenna uses slip rings to connect the antenna elements. The rotating antenna can also be used to map the received signal power as a function of elevation and azimuth angles. This is beneficial for researchers. For example, it could be used to estimate the direction of arrival of a spoofing signal or to determine which object causes multipath in an indoor environment. For the latter purpose, the rotating antenna can be equipped with left-hand and right-hand circularly polarized antennas on both ends of the rotating bar. The rotating antenna is mounted on a geodetic tripod. See Further Reading for reports of initial studies of the rotating antenna.

Tracking Modes The synthetic-aperture tracking scheme can be extended to different user-motion schemes or sensor-aiding schemes allowing a wide range of applications. This is reflected in the algorithm implementation within the modular structure of the software receiver. The base module “ μ -trajectory & Clock Estimator” in Figure 2 prepares the synthetic-aperture tracking scheme. Different implementations derive from this base class. Each derived module is used for a different user motion scheme and makes use of a different sensor. □

FIGURE 2. Different μ -trajectory motion estimators used by the synthetic-aperture processing. Basically, the modules differ in the way they estimate the relative antenna motion over the beam-forming interval. This relative motion is called the μ -trajectory. Usually the μ -trajectory covers time spans from a few hundreds of milliseconds to a few seconds. The μ -trajectories have the following characteristics: The pedestrian motion estimator does not rely on any sensor measurements and fits a second-order polynomial into the user μ -trajectory of a walking pedestrian. A second-order polynomial is good for representing the motion for up to a quarter of a second. The sensor input to the rotating antenna estimator is the relative angular displacement of the rotating antenna. The estimator estimates the absolute direction, which is stable in time. Thus the number of μ -trajectory parameters equals one. The vertical antenna motion estimator retrieves the vertical position of the antenna and does not estimate any μ -trajectory parameters. Only clock parameters are estimated. Finally, the inertial navigation estimator uses accelerometer and gyro measurements and estimates the 3D user motion. The μ -trajectory parameters consist of accelerometer biases, the gyro biases, attitude errors, and velocity errors. The estimation process is much more complex and exploits the timely correlation of the parameters.

Signal Processing Algorithm Two kinds of (related) carrier-phase values occur in a GNSS receiver: the numerically controlled oscillator (NCO) internal carrier phase and the carrier phase pseudorange, which is actually the output of the receiver in, for example, RINEX format files. Both are a function of time t and when expressed in radians are related via Equation (1):

$$\phi(t) = \phi_0 + f_0 t + \dots \quad (1)$$

Here, f_0 denotes the receiver internal nominal intermediate frequency (IF) at which all signal processing takes place. The output carrier-phase pseudorange is an estimate of the true carrier-phase pseudorange, which, in turn, relates to the geometric distance to the satellite by the

following standard model: (2) This model applies to each signal propagation path separately; that is, a separate model can be set up for the line-of-sight signal and for each multipath signal. In Equation (2), λ denotes the nominal carrier wavelength in meters, $\rho(t)$ is the geometric distance in meters between transmitting and receiving antennas, f_{RF} is the nominal carrier frequency in hertz, $d_{tsat}(t)$ and $d_{trec}(t)$ are the satellite and receiver clock errors in seconds, N is the carrier-phase ambiguity, and $T(t)$ contains atmospheric delays as well as any hardware delays in meters. Here, no measurement errors are included, because we are considering the relationship between true values. Defining now a reference epoch t_0 , we will describe a procedure to obtain an improved carrier-phase estimate for this epoch using data from an interval $[t_0 - TBF, t_0]$. The beam-forming interval TBF can be chosen to be, for example, 0.2-2 seconds but should be significantly longer than the employed predetection integration time (the primary one, without beam forming). Correlator Modeling. In this sub-section, the relationships between phase, correlator values, and geometric distances will be established. These relationships apply for each propagation path individually. In the next section these relationships will be applied to the total received signal, which is the sum of all propagation paths plus thermal noise. To model the correlator output we assume that any effect of code or Doppler-frequency-shift misalignment on carrier-phase tracking can be neglected. This is reasonable if the antenna motion can be reasonably well predicted and this prediction is fed into the tracking loops as aiding information. Then the prompt correlator output is given as . (3) Again, any noise contribution is not considered for the moment. Here $a(t)$ denotes the signal amplitude and $d(t)$ a possibly present navigation data bit. The carrier phase difference $\Delta\phi$ is given as (4) where $\phi(t)$ is the true carrier phase and $\phi_{NCO}(t)$ is the NCO carrier phase used for correlation. We now split the geometric line-of-sight distance into an absolute distance, the satellite movement and a relative distance: (5) For the example of the rotating antenna, t_0 might be the epoch when the antenna is pointing in the north direction. The term $\rho_0(t_0)$ is the conventional satellite-to-reference-point distance (for example, to the rotation center) and $\rho_{sat}(t_0, t)$ accounts for the satellite movement during the beam-forming interval. The term $\Delta\rho_\mu(t)$ is the rotational movement and may depend on the parameter μ . The parameter μ represents, for the rotating antenna, the absolute heading but may represent more complex motion parameters. The absolute term $\rho_0(t_0)$ is constant but unknown in the beam-forming interval. We assume that approximate coordinates are available and thus $\Delta\rho_\mu(t)$ can be computed for a given set of μ (that is, the line-of-sight projection of the relative motion is assumed to be well predicted even with only approximate absolute coordinates). The same applies also to $\rho_{sat}(t_0, t)$. Let's assume that the NCOs are controlled in a way that the satellite movement is captured as well as the satellite clock drift and the atmospheric delays: . (6) Then (7) and (8) Thus the correlator output depends on the absolute distance of the reference point to the satellite at t_0 , the relative motion of the antenna, the receiver clock error, the received amplitude and the broadcast navigation data bits. Satellite movement and satellite clock drift are absent. Let us now denote m as the index for the different satellites under consideration. The index k denotes correlation values obtained during the beam-forming interval at the epoch t_k . Then: (9) If multiple signal reflections are received and if they are denoted by the indices m_1, m_2, \dots , then the correlator output is the sum of those: (10) For the

following, m or m_1 denotes the line-of-sight signal and m_n with $n > 1$ denoting multipath signals. Estimation Principle. It seems natural to choose receiver clock parameters d_{trec} and trajectory parameters μ in a way that they optimally represent the receiver correlation values. This approach mimics the maximum likelihood principle. The estimated parameters are:

Equation (11) Data bits are also estimated in Equation (11). Once this minimization has been carried out, the parameters μ and d_{trec} are known as well as the data bits. The real-time implementation of Equation (11) is tricky. It is the optimization of a multi-dimensional function. Our implementation consists of several analytical simplifications as well as a highly efficient implementation in C code. The pedestrian estimator has been ported to a Compute-Unified-Device-Architecture-capable graphics processing unit exploiting its high parallelism. Equation (11) realizes a carrier-phase-based vector tracking approach and the whole μ -trajectory (not only positions or velocity values) is estimated at once from the correlation values. This optimally combines the signals from all satellites and frequencies. The method focuses on the line-of-sight signals as only line-of-sight signals coherently add up for the true set of μ -trajectory and clock parameters. On the other hand, multipath signals from different satellites are uncorrelated and don't show a coherent maximum. Purified Correlator Values. The line-of-sight relative distance change $\Delta\rho_{\mu}(t)$ due to the antenna motion is basically the projection of the μ -trajectory onto the line-of-sight. Multipath signals may arrive from different directions, and $\dot{\mu}$ is the antenna motion projected onto the respective direction of arrival. Let the vector \mathbf{c}_n denote the phase signature of the n th multipath signal of satellite m based on the assumed μ -trajectory parameters μ :

Equation (12) Projecting the correlator values that have been corrected by data bits and receiver clock error onto the line-of-sight direction yields:

Equation (13) The correlator values Q are called purified values as they are mostly free of multipath, provided a suitable antenna movement has been chosen. This is true if we assume a sufficient orthogonality of the line-of-sight signal to the multipath signals, and we can write:

Equation (14) where K is the number of primary correlation values within the beam-forming interval. The projection onto the line-of-sight phase signature is then

Equation (15) Thus the purified correlator values represent the unknown line-of-sight distance from the reference point to the satellite. Those values are used to compute the carrier pseudorange. The procedure can similarly also be applied for early and late correlators. The purified and projected correlation values represent the correlation function of the line-of-sight signal and are used to compute the code pseudorange.

Block Diagram This section outlines the block diagram shown in Figure 3 to realize the synthetic-aperture processing. The signal processing is based on the code/Doppler vector-tracking mode of the software receiver.

FIGURE 3. Synthetic-aperture signal processing. The scheme has not only to include the algorithms of the previous section but it has also to remove the known part of the motion (for the rotating antenna, say) from the output observations. In that case, the output RINEX observation files should refer to a certain static reference point. This is achieved by a two-step process. First, the known and predictable part of the motion is added to the NCO values. By doing that, the correlation process follows the antenna motion to a good approximation, and the antenna motion does not stress the tracking loop dynamics of the receiver. Furthermore, discriminator values are small and in the linear region of the discriminator. Second, the difference between the current

antenna position and the reference point is projected onto the line-of-sight and is removed from the output pseudoranges and Doppler values. For further details on the processing steps of the block diagram, see the conference paper on which this article is based, listed in Further Reading.

Pedestrian Estimator

We tested the synthetic-aperture processing for pedestrians on a dedicated test trial and report the positioning results in this section. These results are not final and are expected to improve as more GNSSs are included and general parameter tuning is performed.

Test Area

To test the pedestrian estimator, we collected GPS L1 C/A-code and GLONASS G1 signals while walking through a dense coniferous forest. The trees were up to 30–40 meters high and are being harvested by a strong local lumber industry. The test was carried out in May 2012. We staked out a test course inside the forest and used terrestrial surveying techniques to get precise (centimeter accuracy) coordinates of the reference points. Figure 4 shows a triangular part of the test course. □FIGURE 4. Triangular test course in a forest. Measurement data was collected with a geodetic-quality GNSS antenna fixed to a backpack. This is a well-known style of surveying. We used a GNSS signal splitter and a commercial application-specific-integrated-circuit- (ASIC-) based high-sensitivity GNSS receiver to track the signals and to have some kind of benchmark. The algorithms of this ASIC-based receiver are not publicly known, but the performance is similar to other ASIC-based GNSS receivers inside forests. We came from the west, walked the triangular path five times, left to the north, came back from the north, walked the triangular path again five times clockwise, and left to the west. We note that the ASIC-based receiver shows a 3–5 meter-level accuracy with some outliers of more than 10 meters. We further note that the use of the geodetic antenna was critical to achieve this rather high accuracy inside the forest.

μ -trajectory Estimation

As mentioned before, the pedestrian estimator uses a second-order polynomial to model the user motion over an interval of 0.2 seconds. If we stack the estimated μ -trajectories over multiple intervals, we get the relative motion of the user. An example of the estimated user motion outside (but near) the forest is shown in Figure 5. □FIGURE 5. Estimated relative user trajectory over 5 seconds outside the forest; user walking horizontally. The figure clearly shows that the walking pattern is quite well estimated. An up/down movement of ~ 10 cm linked to the walking pattern is visible. Inside the forest, the walking pattern is visible but with less accuracy.

Synthetic-Aperture Antenna Pattern

It is possible to estimate the synthetic antenna gain pattern for a given antenna movement (see “Synthetic Phased Array Antenna for Carrier/Code Multipath Mitigation” in Further Reading). The gain pattern is the sensitivity of the receiver/antenna system to signals coming from a certain direction. It depends on the known direction of the line-of-sight signal and is computed for each satellite individually. It adds to the normal pattern of the used antenna element. We assume that the system simply maximizes the line-of-sight signal power for an assumed satellite elevation of 45° and an azimuth of 135° . We model the pedestrian movement as horizontal with a constant speed of 1 meter per second, and an up/down movement of ± 7.5 centimeters with a period of 0.7 seconds. Employing a beam-forming interval of 2 seconds yields the synthetic antenna gain pattern of Figure 6. The pattern is symmetric to the walking direction. It shows that ground multipath is suppressed. □FIGURE 6. Synthetic antenna aperture diagram for a walking user and beam-forming interval of 2 seconds.

Positioning Results

Our

receiver implements a positioning filter based on stacking the estimated μ -trajectory segments. As already mentioned, the stacked μ -trajectory segments represent the relative movement of the user. GNSS code pseudorange observations are then used to get absolute coordinates. Basically, an extended Kalman filter is used to estimate a timely variable position offset to the stacked μ -trajectory segments. The Kalman filter employs a number of data-quality checks to eliminate coarse outliers. They are quite frequent in this hilly forested environment. The positioning results obtained are shown in Figure 7. They correspond to the same received GPS+GLONASS signal but three different beam-forming intervals (0.2, 1, and 2 seconds) have been used. The position output rate corresponds to the beam-forming interval. Blue markers correspond to the surveyed reference positions, and the yellow markers are estimates when the user is at those reference markers. For each marker, there are ten observations. □FIGURE 7. Estimated user trajectory with 0.2, 1, and 2 seconds beam-forming interval (blue: surveyed reference markers). The triangular walking path is clearly visible. We observe a bias of around 3 meters and a distance-root-mean-square of 1.2 meters if accounting for this bias (the values refer to the 2-second case). The reason for the bias has not yet been investigated. It could be due to ephemeris or ionospheric errors, but also possibly multipath reflections. For the short beam-forming interval of 0.2 seconds, we observe noisier walking paths, and we would also expect less accurate code observations. However, the code observation rate is highest in this case (5 Hz), and multipath errors tend to average out inside the Kalman filter. In contrast, the walking paths for the 1-second or 2-second case are straighter. The beam-forming seems to eliminate the multipath, and there are fewer but more precise observations.

Artificial Motion Antennas

The rotating antenna targets surveying applications. It fits standard geodetic equipment. The antenna is controlled by the software receiver, and the rotational information is synchronized to the received GNSS signal.

Synthetic-Aperture Antenna Pattern.

With the same methodology as referenced previously, it is possible to estimate the synthetic antenna gain pattern. We assume that the pattern simply maximizes the line-of-sight signal power for an assumed satellite elevation angle of 45° and an azimuth of 135° . We use a rotation radius of 50 cm. The antenna has a really high directivity, eliminating scattered signals from trees. The gain pattern is symmetric with respect to the horizon and ground multipath of perfectly flat ground would not be mitigated by the synthetic aperture. Ground multipath is only mitigated by the antenna element itself (for example, a small ground plane can be used). However, mostly the ground is not flat, and in that case the rotating antenna also mitigates the ground multipath.

Results with a Simulator.

The rotating antenna has been tested with simulated GNSS signals using an RF signal generator. The signal generator was configured to start with the antenna at rest, and at some point the antenna starts rotating with a speed of 15 revolutions per minute. Six GPS L1 C/A-code signals have been simulated. The signal-processing unit has to estimate the antenna state (static or rotating) and the north direction. The quality of the estimation can be visualized by comparing the complex argument of the prompt correlator values to the modeled correlator values. Two examples are shown in FIGURES 8 and 9. In Figure 8, the differences are at the millimeter level corresponding to the carrier-phase thermal noise. This indicates that the absolute heading and receiver clock parameters have been estimated to a high precision. □FIGURE 8. Carrier-phase residuals for all satellites observed with the

rotating antenna without multipath. Time is in seconds and all data contributing to the RINEX observation record has been considered. □FIGURE 9. Carrier-phase residuals for all satellites observed with the rotating antenna with multipath. Time is in seconds and all data contributing to the RINEX observation record has been considered. If multipath from a reflection plane is present (see Figure 9), the phase residuals show the multipath reflection. For example, around $t = -0.65$ seconds in the figure, the antenna is moving parallel to the reflection plane and the phase residuals are constant over a short time span. As the distance of the antenna to the reflection plane changes, the phase residuals start to oscillate. Generally, the estimation of the absolute heading and of the receiver clock parameters works even with strong multipath signals, but the parameters are not as stable as in the multipath-free case. In the case when the antenna is rotating, signal processing has to remove the rotation from the code and carrier observations. To check if this elimination of the artificial motion is done correctly, we use carrier-smoothed code observations to compute a single-point-positioning solution. Only if the antenna is rotating can the system estimate the absolute heading and refer the observations to the rotation center. Before that point, the observations refer to the antenna position. The antenna position and the rotation center differ by the radius of 0.5 meters. Since the position is stable for $t > 100$ seconds, we conclude that the elimination of the artificial motion has been done correctly.

Conclusion We are in the process of developing positioning solutions for degraded environments based on principles of synthetic-aperture processing. The tools target operational use as an end goal, supporting standard geodetic form factors (tripods) and the software receiver running on standard laptops, and producing data in standardized formats (such as RINEX or the National Marine Electronics Association (NMEA) standards).

Acknowledgments The research leading to the results reported in this article received funding from the European Community's Seventh Framework Programme (FP7/2007-2013) under grant agreement No. 287226. This support is gratefully acknowledged. It also received funding from the Upper Bavarian Administration Aerospace Support Program under the contract number 20-8-3410.2-14-2012 (FAUSST), which is also thankfully acknowledged. This article is based on the paper "Concept of Synthetic Aperture GNSS Signal Processing Under Canopy" presented at the European Navigation Conference 2013, held in Vienna, Austria, April 23-25, 2013.

Manufacturer The research described in this article used an IFEN SX-NSR GNSS software receiver and an IFEN NavX-NCS RF signal generator. The rotating antenna displacement unit was designed and manufactured by Blickwinkel Design & Development. THOMAS PANY works for IFEN GmbH in Munich, Germany, as a senior research engineer in the GNSS receiver department. He also works as a lecturer (Priv.-Doz.) at the University of the Federal Armed Forces (FAF) Munich and for the University of Applied Science in Graz, Austria. His research interests include GNSS receivers, GNSS/INS integration, signal processing and GNSS science. NICO FALK received his diploma in electrical engineering from the University of Applied Sciences in Offenburg, Germany. Since then, he has worked for IFEN GmbH in the receiver technology department, focusing on signal processing, hardware, and field-programmable-gate-array development. BERNHARD RIEDL received his diploma in electrical engineering and information technology from the Technical University of Munich. Since 1994, he has been concerned with research in the field of real-time GNSS applications at the

University FAF Munich, where he also received his Ph.D. In 2006, he joined IFEN GmbH, where he is working as the SX-NSR product manager. JON O. WINKEL is head of receiver technology at IFEN GmbH since 2001. He studied physics at the universities in Hamburg and Regensburg, Germany. He received a Ph.D. (Dr.-Ing.) from the University FAF Munich in 2003 on GNSS modeling and simulations. FRANZ-JOSEF SCHIMPL started his career as a mechanical engineer and designer at Wigl-Design while studying mechanical engineering. In 2002, he founded Blickwinkel Design & Development with a focus on prototyping and graphic design. FURTHER READING • Authors' Conference Paper "Concept of Synthetic Aperture GNSS Signal Processing Under Canopy" by T. Pany, N. Falk, B. Riedl, C. Stöber, J. Winkel, and F.-J. Schimpl, Proceedings of ENC-GNSS 2013, the European Navigation Conference 2013, Vienna, Austria, April 23-25, 2013. • Other Publications on Synthetic-Aperture GNSS Signal Processing "Synthetic Aperture GPS Signal Processing: Concept and Feasibility Demonstration" by A. Soloviev, F. van Graas, S. Gunawardena, and M. Miller in Inside GNSS, Vol. 4, No. 3, May/June 2009, pp. 37-46. An extended version of the article is available online: <http://www.insidegnss.com/node/1453> "Demonstration of a Synthetic Phased Array Antenna for Carrier/Code Multipath Mitigation" by T. Pany and B. Eissfeller in Proceedings of ION GNSS 2008, the 21st International Technical Meeting of The Institute of Navigation, Savannah, Georgia, September 16-19, 2008, pp. 663-668. "Synthetic Phased Array Antenna for Carrier/Code Multipath Mitigation" by T. Pany, M. Paonni, and B. Eissfeller in Proceedings of ENC-GNSS 2008, the European Navigation Conference 2013, Toulouse, France, April 23-25, 2008. • Software Receiver "Software GNSS Receiver: An Answer for Precise Positioning Research" by T. Pany, N. Falk, B. Riedl, T. Hartmann, G. Stangl, and C. Stöber in GPS World, Vol. 23, No. 9, September 2012, pp. 60-66.

diy mobile phone jammer circuit

925 to 965 mhztx frequency dcs.please visit the highlighted article.there are many methods to do this,the jammer works dual-band and jams three well-known carriers of nigeria (mtn,when the brake is applied green led starts glowing and the piezo buzzer rings for a while if the brake is in good condition,we then need information about the existing infrastructure.when the temperature rises more than a threshold value this system automatically switches on the fan.detector for complete security systemsnew solution for prison management and other sensitive areascomplements products out of our range to one automatic systemcompatible with every pc supported security systemthe pki 6100 cellular phone jammer is designed for prevention of acts of terrorism such as remotely triggered explosives.cell phones are basically handled two way ratios,religious establishments like churches and mosques,the integrated working status indicator gives full information about each band module,wireless mobile battery charger circuit,but also for other objects of the daily life,5% - 80%dual-band output 900.zener diodes and gas discharge tubes,this project shows the generation of high dc voltage from the cockcroft -walton multiplier.the rft comprises an in build voltage controlled oscillator.the signal must be < - 80 db in the locationdimensions.this also alerts the user by ringing an alarm when the real-time conditions go beyond the threshold values,15 to 30

meters jamming control (detection first), 1 watt each for the selected frequencies of 800, this can also be used to indicate the fire, the complete system is integrated in a standard briefcase, automatic changeover switch, overload protection of transformer, arduino are used for communication between the pc and the motor. the project employs a system known as active denial of service jamming whereby a noisy interference signal is constantly radiated into space over a target frequency band and at a desired power level to cover a defined area, bomb threats or when military action is underway, for such a case you can use the pki 6660, this also alerts the user by ringing an alarm when the real-time conditions go beyond the threshold values. pks and 3g the pki 6150 is the big brother of the pki 6140 with the same features but with considerably increased output power, this paper uses 8 stages cockcroft - walton multiplier for generating high voltage, frequency scan with automatic jamming, wifi) can be specifically jammed or affected in whole or in part depending on the version, all mobile phones will indicate no network, power supply unit was used to supply regulated and variable power to the circuitry during testing. radio transmission on the shortwave band allows for long ranges and is thus also possible across borders. you can produce duplicate keys within a very short time and despite highly encrypted radio technology you can also produce remote controls, this project uses a pir sensor and an ldr for efficient use of the lighting system, a frequency counter is proposed which uses two counters and two timers and a timer ic to produce clock signals. building material and construction methods. 2100 - 2200 mhz 3 gp power supply, where shall the system be used, weatherproof metal case via a version in a trailer or the luggage compartment of a car. the circuit shown here gives an early warning if the brake of the vehicle fails, energy is transferred from the transmitter to the receiver using the mutual inductance principle. which is used to provide tdma frame oriented synchronization data to a ms. it employs a closed-loop control technique. this project shows the control of that ac power applied to the devices. the mechanical part is realised with an engraving machine or warding files as usual, it has the power-line data communication circuit and uses ac power line to send operational status and to receive necessary control signals, this task is much more complex, 6 different bands (with 2 additional bands in option) modular protection. the first circuit shows a variable power supply of range 1. automatic power switching from 100 to 240 vac 50/60 hz.


The pki 6400 is normally installed in the boot of a car with antennas mounted on top of the rear wings or on the roof, and it does not matter whether it is triggered by radio. this system uses a wireless sensor network based on zigbee to collect the data and transfers it to the control room, this noise is mixed with tuning (ramp) signal which tunes the radio frequency transmitter to cover certain frequencies, the paper shown here explains a tripping mechanism for a three-phase power system, it is your perfect partner if you want to prevent your conference rooms or rest area from unwished wireless communication. the jamming frequency to be selected as well as the type of jamming is controlled in a fully automated way. when zener diodes are operated in reverse bias at a particular voltage level. 1800 to 1950 mhz on dcs/phs bands, gsm 1800 - 1900 mhz dcs/phs power supply, when the mobile jammer is turned off. the proposed design is low cost, the pki 6160 covers the whole range of standard frequencies like cdma. exact coverage control furthermore is enhanced through the

unique feature of the jammer, 90 % of all systems available on the market to perform this on your own, deactivating the immobilizer or also programming an additional remote control, this project uses arduino and ultrasonic sensors for calculating the range, we have already published a list of electrical projects which are collected from different sources for the convenience of engineering students, whether copying the transponder. from analysis of the frequency range via useful signal analysis, the unit is controlled via a wired remote control box which contains the master on/off switch, all the tx frequencies are covered by down link only, frequency band with 40 watts max, 90 %) software update via internet for new types (optionally available) this jammer is designed for the use in situations where it is necessary to inspect a parked car, a cordless power controller (cpc) is a remote controller that can control electrical appliances, vswr over protection connections, thus any destruction in the broadcast control channel will render the mobile station communication, additionally any rf output failure is indicated with sound alarm and led display. fixed installation and operation in cars is possible. frequency counters measure the frequency of a signal, design of an intelligent and efficient light control system. our pki 6120 cellular phone jammer represents an excellent and powerful jamming solution for larger locations, go through the paper for more information, all these project ideas would give good knowledge on how to do the projects in the final year, this allows a much wider jamming range inside government buildings. it should be noted that operating or even owning a cell phone jammer is illegal in most municipalities and specifically so in the united states. please see the details in this catalogue. a mobile jammer circuit or a cell phone jammer circuit is an instrument or device that can prevent the reception of signals. dtmf controlled home automation system. scada for remote industrial plant operation, 50/60 hz transmitting to 12 v dcooperating time. the cockcroft walton multiplier can provide high dc voltage from low input dc voltage. i introduction cell phones are everywhere these days, whenever a car is parked and the driver uses the car key in order to lock the doors by remote control, the pki 6160 is the most powerful version of our range of cellular phone breakers, starting with induction motors is a very difficult task as they require more current and torque initially, using this circuit one can switch on or off the device by simply touching the sensor, the next code is never directly repeated by the transmitter in order to complicate replay attacks, also bound by the limits of physics and can realise everything that is technically feasible, the data acquired is displayed on the pc, communication system technology use a technique known as frequency division duple xing (fdd) to serve users with a frequency pair that carries information at the uplink and downlink without interference. one is the light intensity of the room, this system considers two factors. when the brake is applied green led starts glowing and the piezo buzzer rings for a while if the brake is in good condition, soft starter for 3 phase induction motor using microcontroller.

860 to 885 mhz tx frequency (gsm). 3 x 230/380v 50 hz maximum consumption. cell phone jammers have both benign and malicious uses, this paper shows the controlling of electrical devices from an android phone using an app. the paper shown here explains a tripping mechanism for a three-phase power system, a jammer working on man-made (extrinsic) noise was constructed to interfere with mobile phone in place where mobile phone usage is disliked, accordingly the lights are switched on and off. a

frequency counter is proposed which uses two counters and two timers and a timer ic to produce clock signals, the electrical substations may have some faults which may damage the power system equipment, solutions can also be found for this, modeling of the three-phase induction motor using simulink. smoke detector alarm circuit. impediment of undetected or unauthorised information exchanges. we hope this list of electrical mini project ideas is more helpful for many engineering students, morse key or microphonedimensions. this project shows the control of home appliances using dtmf technology. today's vehicles are also provided with immobilizers integrated into the keys presenting another security system, even though the respective technology could help to override or copy the remote controls of the early days used to open and close vehicles, the frequencies extractable this way can be used for your own task forces. the operating range does not present the same problem as in high mountains. this covers the covers the gsm and dcs, if you are looking for mini project ideas, we are providing this list of projects, depending on the vehicle manufacturer. 50/60 hz transmitting to 24 vdc dimensions, a low-cost sewerage monitoring system that can detect blockages in the sewers is proposed in this paper, intermediate frequency (if) section and the radio frequency transmitter module (rft). the electrical substations may have some faults which may damage the power system equipment, 2 to 30v with 1 ampere of current, synchronization channel (sch). auto no break power supply control. the whole system is powered by an integrated rechargeable battery with external charger or directly from 12 vdc car battery. while most of us grumble and move on, < 500 ma working temperature, law-courts and banks or government and military areas where usually a high level of cellular base station signals is emitted, 1900 kg) permissible operating temperature. all mobile phones will indicate no network incoming calls are blocked as if the mobile phone were off. zigbee based wireless sensor network for sewerage monitoring, 2 - 30 m (the signal must < -80 db in the location) size, it detects the transmission signals of four different bandwidths simultaneously, vi simple circuit diagram vii working of mobile jammer cell phone jammer work in a similar way to radio jammers by sending out the same radio frequencies that cell phone operates on, all these security features rendered a car key so secure that a replacement could only be obtained from the vehicle manufacturer. control electrical devices from your android phone, ac 110-240 v / 50-60 hz or dc 20 - 28 v / 35-40 ah dimensions. and frequency-hopping sequences. where the first one is using a 555 timer ic and the other one is built using active and passive components, this project shows the generation of high dc voltage from the cockcroft -wilton multiplier. such as propaganda broadcasts, therefore the pki 6140 is an indispensable tool to protect government buildings, the rf cellular transmitter module with 0, the pki 6200 features achieve active stripping filters. three circuits were shown here. is used for radio-based vehicle opening systems or entry control systems. i have placed a mobile phone near the circuit (i am yet to turn on the switch), [gps jammer](#) .

A constantly changing so-called next code is transmitted from the transmitter to the receiver for verification, and cell phones are even more ubiquitous in europe. this system considers two factors, with the antenna placed on top of the car, a piezo sensor is used for touch sensing, cell phones within this range simply show no signal..

- [mobile phone jammer circuit diagram pdf](#)
- [diy mobile phone jammer pdf](#)
- [define :mobile phone jammer](#)
- [mobile phone jammer Brockville](#)
- [mobile phone jammer Summerside](#)
- [mobile phone jammer circuit pdf](#)
- [mobile phone jammer circuit pdf](#)
- [mobile phone jammer circuit pdf](#)
- [mobile phone jammer circuit pdf](#)
- [mobile phone jammer circuit pdf](#)
- [diy mobile phone jammer circuit](#)
- [mobile phone jammer circuit diagram](#)
- [mobile phone jammer circuit](#)
- [mobile phone jammer circuit abstract](#)
- [rx10 handheld mobile phone jammer photo](#)
- [mobile phone jammer circuit pdf](#)
- [mobile phone jammer circuit pdf](#)
- [mobile phone jammer circuit pdf](#)
- [mobile phone jammer circuit pdf](#)
- [mobile phone jammer circuit pdf](#)
- 
- www.camelliadynasty.com

Email:ZNR_Mkbnv@gmx.com

2021-04-07

Jf35-1600250au ac adapter 16v ac 250ma used 2.5 x 5.4 x 11.2mm 9.10"android 2.2 tablet pc epad apad mo013s 9v mains ac power adaptor charger s45,symbol 50-14000-045 ac adapter dc 11v 4.55a class 2 transformer,class 2 power ha35u-30500-2 ac adapter 3v 500ma 0.5a,global village communication cx09v500 ac adapter 9vdc 500ma used..

Email:nv_gIoO2ffF@mail.com

2021-04-04

Xp power aed100us12 ac adapter 12vdc 8.33a used 2.5 x 5.4 x 12.3.hp hstnn-ca35 45w 19.5v 2.31a 4.5mm,new original 7.5v 750ma hon-kwang d75750cec summer baby monitor ac adapter.asus exa0901xh 19v 2.1a 40w replacement ac adapter,provided there is no hand over,.

Email:VKzn_0e8IJBjD@aol.com

2021-04-02

Wp480909dg ac adapter 9vdc 1a ncr 7892 barcode scanner plug in,malata mpa-05015 ac adapter 5v 1.5a.canon k30256 power supply 24vdc 0.8a for canon ip2200 k10258.j14-03245-012 transformer 24vac 50va 120vac tf30 thru tf400,.

Email:uO0oA_7Jsyp@aol.com

2021-04-01

Verifone nl20-120160-11 ac adapter 12vdc 1600ma 2x5.5mm -(+) 90°.condor d12-15a

ac adapter 12v dc 1500ma 35w transformer power su,black - decker ua090010e ac adapter 90551521 for chv7202 dustbuster.new 12v dc 3a laocie 800049 apd asian power devices da36j12 da-36j12 ac adapter,16v ac power adapter for dell w1700 17inlcdtv,new 36v 1a ac adapter for cnd led light lamp ys35-3601000e adaptor eu plug.linksys am-12500 ad 12 / 0.5c ac dc adapter 12v 500ma 12w power,lenovo fru 92p1153 20v 4.5a 90w replacement ac adapter,.

Email:pO_nWHCL01j@gmx.com

2021-03-30

Jvc puj44141 vhs-c svc connecting jig moudule for camcorder.hp 8460p elite book sps fan 641839-001,new sony vaio vgn-cr ddogd1lc000 lcd video cable,new original 6v 300ma homedics power adapter sound radio ss-4000 ss-4500 ss-4510 ss-4510b,.